HHS Public Access

Author manuscript

*J Periodontol*. Author manuscript; available in PMC 2023 February 15.

Published in final edited form as:

*J Periodontol*. 2020 May ; 91(5): 671–682. doi:10.1002/JPER.18-0748.

# `TLR4 mediates alveolar bone resorption in experimental peri-implantitis through regulation of CD45+ cell infiltration, RANKL/OPG ratio, and inflammatory cytokine production

**Shu Deng**[1,2], **Yang Hu**[1,3], **Jing Zhou**[1,3], **Yufeng Wang**[1,4,5], **Yuguang Wang**[6], **Sicong Li**[1,3], **Grace Huang**[1], **Cheng Peng**[2], **Anka Hu**[1], **Qing Yu**[1,3], **Xiaozhe Han**[1,3]

[1]Department of Immunology and Infectious Diseases, The Forsyth Institute, Cambridge, Massachusetts, USA

[2]Department of Stomatology, The secondary Hospital of Tianjin Medical University, Tianjin, China

[3]Oral Medicine, Infection, and Immunity, Harvard School of Dental Medicine, Boston, Massachusetts, USA

[4]Department of Oral Mucosal Diseases, Ninth People's Hospital, College of Stomatology, Shanghai Jiaotong University School of Medicine, Shanghai, China

[5]Shanghai Key Laboratory of Stomatology & Shanghai Research Institute of Stomatology, Shanghai, China

[6]Center of Digital Dentistry, Peking University School and Hospital of Stomatology, Beijing, China

## Abstract

**Background:** The present study was to determine the role of Toll-like receptor 4 (TLR4) signaling in inflammation and alveolar bone resorption using a murine model of *Porphyromonas gingivalis*-associated ligature-induced peri-implantitis.

**Methods:** Smooth surface titanium implants were placed in the left maxilla alveolar bone 6 weeks after extraction of first and second molars in Wild-type (WT) and TLR4$^{-/-}$ (TLR4 KO) mice. Silk ligatures immersed with *P. gingivalis* were tied around the implants 4 weeks after the implant placement and confirmation of osteointegration. Two weeks after the ligation,

**Correspondence:** Dr. Xiaozhe Han, The Forsyth Institute, Department of Immunology and Infectious Diseases, 245 First Street, Cambridge, MA 02142, USA, xhan@forsyth.org.

AUTHOR CONTRIBUTIONS

Shu Deng contributed to conception and design, contributed to acquisition, analysis, and interpretation, drafted manuscript; Yang Hu contributed to conception and design, contributed to acquisition, analysis, and interpretation, drafted manuscript, and critically revised the manuscript for important intellectual content; Jing Zhou, contributed to acquisition, analysis, and interpretation; Yufeng Wang contributed to acquisition, analysis, and interpretation; Yuguang Wang contributed to acquisition, analysis, and interpretation; Sicong Li contributed to acquisition, analysis, and interpretation; Grace Huang contributed to acquisition, analysis, and interpretation; Cheng Peng contributed to acquisition, analysis, and interpretation; Anka Hu contributed to acquisition, analysis, and interpretation; Qing Yu critically revised the manuscript for important intellectual content; and Xiaozhe Han contributed to conception and design, contributed to acquisition, analysis, and interpretation, critically revised the manuscript for important intellectual content, and agreed to be accountable for all aspects of the work in ensuring that questions relating to the accuracy or integrity of any part of the work are appropriately investigated and resolved.

The authors report no conflicts of interest related to this study.

SUPPORTING INFORMATION

Additional supporting information may be found online in the Supporting Information section at the end of the article.

bone resorption, osteoclastogenesis, cellular inflammatory responses, and gingival mRNA expression levels of cytokines were assessed by micro-computed tomography, tartrate-resistant acid phosphatase (TRAP) staining, immunobiological examination and Real-time quantitative polymerase chain reaction, respectively.

**Results:** In both WT and TLR4 KO mice, the bone resorption around implants was significantly increased in the *P. gingivalis*/ligation group compared with control group. In *P. gingivalis*/ligation group, the levels of bone resorption, TRAP+ cell formation, and gingival CD3+ and CD45+ cell infiltration were significantly decreased in TLR4 KO mice compared with that in WT mice. Receptor activator of nuclear factor-kappa B ligand /osteoprotegerin (RANKL/OPG) ratio was significantly increased after *P. gingivalis*/ligation treatment in WT mice not in TLR4 KO mice. When comparing the *P. gingivalis*/ligation group with the respective control group, gingival mRNA expressions of IL-1$\beta$, IFN-$\gamma$, and 1L-17 were significantly increased in TLR4 KO mice.

**Conclusion:** This study suggests that TLR4 mediates alveolar bone resorption in *P. gingivalis* associated ligature-induced peri-implantitis through regulation of immune B cell infiltration, RANKL/OPG expression ratio, and differential inflammatory cytokine production.

### Keywords

bone resorption; peri-implantitis; TLR4

## 1 | INTRODUCTION

Tooth loss is a common complication for people all over the world and negatively affects one's life.[1] Dental implant has become a preferable choice to restore the missing tooth in the past some decades for functional and esthetic purposes.[2] However, peri-implantitis has become prevalent accompanying the exponential growth of dental implant procedures.[3] Current treatment available for peri-implantitis is not satisfactory due to the lack of understanding of the disease pathogenesis.[4] Some suggested that periodontitis and peri-implantitis shares similar features associated with bacterial infection and the host immune responses,[5] while others indicated that the two diseases show distinctive characteristics when compared with each other, although not all of them are human studies.[6–9] Despite clinical data analysis and scientific reports, the mechanism of peri-implantitis pathogenesis still remains unclear.[10,11]

Toll-like receptors are a family of well-characterized pattern recognition receptors and play an important role in the induction of proinflammatory cytokines by recognizing the signature molecules of the host innate immunity.[12,13] Toll-like receptor 4 (TLR4) is reported to involve in the acceleration of the bone resorption in periodontitis[14] and involved in the host immune responses to Gram-negative bacteria by recognizing their outer membrane component lipopolysaccharide (LPS).[15] However, the role of TLR4 in peri-implantitis remains unknown.

*Porphyromonas gingivalis*, a Gram-negative anaerobic bacteria, is reported to be involved in the progress of periodontitis and peri-implantitis by clinical and biologic studies.[16,17] Our previously studies indicated that TLR4 could recognize the surface components of

*P. gingivalis* and promote the proinflammatory cytokine responses and osteoclastogenesis in *P. gingivalis* associated ligature induced periodontitis.[18] Moreover, *P. gingivalis*-induced periodontal bone resorption is TLR4-dependent.[19] The purpose of this study is to determine the role of TLR4 signaling in peri-implantitis inflammation and bone loss and its associated cellular and molecular mechanism, using a mouse model of *P. gingivalis*-associated ligature induced experimental peri-implantitis. In the current model, live *P. gingivalis* infection was used to establish relevance to human disease and ligation was used to facilitate biofilm accumulation and bacterial colonization around implant.

## 2 | MATERIALS AND METHODS

### 2.1 | Bacterial culture

*P. gingivalis* (strain ATCC 33277) was recovered and grown on anaerobic blood agar plates* in an anaerobic hood with 85% N2, 5% H2, and 10% CO2. The bacteria was transferred to a new plate every 7 days after the recovery. After transferring three times, a single colony of *P. gingivalis* was isolated and grown in Trypticase soy broth† containing 5 μg/mL hemin and vitamin K. Bacterial numbers were checked by a spectrophotometer before use. An equal volume of sterile 2% (wt/vol) low-viscosity carboxymethyl cellulose was mixed together with the bacteria suspension to facilitate the local colonization of the bacteria.

### 2.2 | Animals

Wild-type (WT) and TLR4 KO mice in C57/BL6 background (4 weeks old, male: female = 1:1) were purchased.‡ All the animal associated protocols were reviewed and approved by the Institutional Animal Care and Use Committee of the Forsyth Institute (#18–004). The mice were maintained in specific pathogen-free environment and fed with soft diet *ad libitum* during the experiment under 12 hours light- and 12 hours dark-cycle. A total of four groups were included in the study, which contain control and experimental groups for both WT and TLR4 KO mice (n = 12 for each group, six mice were used for histology study and six mice were used for mRNA expression analysis).

### 2.3 | Tooth extraction, implant placement, and peri-implantitis induction by *P. gingivalis* associated ligature

The procedures of tooth extraction and implants placement were as previously described.[9] Briefly, all the mice had their left maxillary first and second molars extracted at 4 weeks old with 6 weeks of healing time after the tooth extraction. Drinking water with antibiotics (sulfamethoxazole and trimethoprim, 850 μg/170 μg/mL) was used to decrease the possibility of infection after tooth extraction for 4 weeks. The maxillary alveolar bone was drilled with the 0.3 mm-diameter carbide micro-hand drill. A smooth-surface, screw-shaped titanium implant§ (1 mm in length and 0.5 mm in diameter) was screwed clockwise into the bone through the drilled site until torque can be achieved. Antibiotics were given for 1 week after implantation and 4 weeks of healing time followed implant placement. Four

*NHK agar, Northeast Laboratory Services, Waterville, ME.
†BD Biosciences, San Diego, CA.
‡Jackson lab, Bar Harbor, ME.
§D.P. Machining, La Verne, CA.

weeks later, a 7–0 silk ligature was tied around the implants in mice after being soaked in the *P. gingivalis* suspension for 30 minutes.

### 2.4 | Tissue collection and sample preparation

The ligatures were maintained for another 2 weeks, after which the mice were euthanized by $CO_2$ inhalation and the maxilla were harvested. The gingival tissues were extracted and collected from six WT and six TLR4 KO mice for RNA isolation. The skulls were then defleshed by beetles for 1 week followed by$H_2O_2$ (3%) bleaching for 4 hours. Bone resorption was measured by microscope imaging analysis and microcomputed tomography (μCT) scan analysis. The other six maxilla from WT and TLR4 KO mice were fixed in formalin overnight in 4°C followed by EDTA decalcification for 3 weeks. All the decalcification samples were embedded into optimal cutting temperature (OCT) compound and then stored in −80°C. All the sections were cut in 8 μm sections by Cryotome and then subjected to immunohistological analysis.

### 2.5 | Imaging analysis for bone resorption

The bone resorption measurements were assessed under a Microscope* and analyzed by software Image-J (National Institutes of Health [NIH]) as previously described[20] and modified. Briefly, the region of interest (ROI) of the bone resorption area was defined as coronally by the lower edge of the implants, laterally by the mesial and distal outline of the implant and the apically by the alveolar crest. All the defleshed skulls were also scanned with a high-resolution microcomputed tomography scanner.† Seg3D software was used to establish the quantitative three dimensional (3-D) images and followed by the measurements of the bone resorption volume as previously described.[9]

### 2.6 | Hematoxylin and eosin (H&E) staining, tartrate-resistant acid phosphatase (TRAP) staining, and immunofluorescence (IF) staining

All the maxilla collected were fixed in 4% formaldehyde overnight and then went through decalcification in 10% EDTA for 3 weeks in 4°C with shaking. Eight-micron-thick sections were produced in the mesial-distal plane for H&E, TRAP, and IF staining. For H&E staining, images were analyzed by Image-J after being captured by a digital camera. The numbers of inflammatory cells in gingival tissues surrounding the implant on each section (six sections per sample) were counted at magnification of 40× and the average number was calculated. An acid phosphatase kit‡ was used for TRAP staining. After 30 minutes staining and 1 minute counterstain with hematoxylin, we counted TRAP positive cells along the alveolar bone surface with ≥3 nuclei which were considered osteoclasts as previously described.[9] A region of interest (ROI) was defined in peri-implantitis samples as: a 1.5 × 1 mm rectangular area aligned with the central long axis of the implant and covered the entire length of the implant. Each section was acquired under light microscope at objective magnification 40×.Osteoclast numbers within the ROI were quantified manually by Image-J. For immunofluorescence (IF) staining, the process was carried similarly as described in

*Nikon SMZ745T, Nikon Instruments, Japan.
†mCT-40, Scanco Medical, Sweden.
‡387A, Sigma, St. Louis, MO.

our previously study.[21] Briefly, all the sections were blocked by 1% bovine serum albumin (BSA) for 1 hour in room temperature. A rat anti-mouse CD45, a rat anti-mouse CD3, and a rabbit anti-mouse RANKL antibodies were applied for 2 hours at room temperature according to the manufacturer's instruction. A secondary fluorescence-labeled goat anti-rat immunoglobulin G and goat anti-rabbit immunoglobulin G were applied on the slides for 1 hour. DAPI (4′,6-diamidino-2-phenylindole) was used to counterstain cells for 30 seconds. Images were taken with a confocal microscope system to detect the CD3-, CD45-, and RANKL- positive cells in the gingival tissues at the mesial and distal edge of the implant-bone interface. The positive cell numbers were analyzed and averaged from 4 to 5 serial sections per sample (six fields per section).

### 2.7 | RNA extraction, reverse transcription, and real time quantitative PCR (RT-qPCR)

Palatal gingival tissues were isolated from around the implants and processed to extract RNA as previously described.[20] Briefly, 2 mm-palatal gingival collar around the implant was collected under a surgical microscope and homogenized in lysis buffer using a tissue homogenizer. Total RNA was extracted, homogenized gingival tissue using RNA extraction kit.[§] cDNA was generated using the SuperScript II Reversed Transcriptase kit*** according to the manufacturer's protocol. The mRNA level of IL-1$\beta$, TNF-$\alpha$, IL-6, IL-10, IL-17A, IFN-$\gamma$, RANKL, and osteoprotegerin (OPG) in gingival tissue were detected by RT-qPCR with SYBR Green I Master Kit in a real-time PCR system.[¶] The sequences of primers were shown in Table 1. GAPDH gene was used as housekeeping gene.

### 2.8 | Statistical analysis

Results were presented as mean ± SEM. Unpaired Student *t*-test was used to analyze differences between any two groups of data sets. For Student *t*-test, the Bonferroni correction was applied after normality test for the data distribution. Results with $P < 0.05$ are considered statistically significant.

## 3 | RESULTS

### 3.1 | *P. gingivalis* infection plus ligation induced peri-implant inflammation and bone loss in mice

Overall, 91.6% (22 out of 24) implants in WT mice achieved osteointegration (no mobility when touched by needles, no obvious bleeding on probing) after being placed for 1 week, after which none of the implants failed. The gingival tissue surrounding the implant appeared healthy (pink in color, no obvious swelling, no bleeding on probing) 4 weeks after implant placement in WT mice (Fig. 1). However, significantly higher level of bleeding sites on probing around implant was found in the ligation group compared with the control group ($P < 0.01$, see Supplementary Table 1 in online *Journal of Periodontology*). Furthermore, ligation group showed a significantly greater bone resorption compared with control group in WT mice, for both 2D imaging analysis ($P = 0.0044$, Figs. 2A and 2E) and 3D μCT analysis ($P = 0.0088$, Figs. 2B and 2F). These results indicate that *P. gingivalis*-soaked

[§]Qiagen Inc, Germantown, MD.
[¶]LightCycler 480, Roche Molecular Systems, Branchburg, NJ.

ligature successfully induced inflammation and bone resorption in this mouse model of experimental peri-implantitis.

### 3.2 | The severity of gingival inflammation was reduced in TLR4 KO mice compared with WT mice after *P. gingivalis* infection plus ligation

Overall, 87.5% (21 out of 24) implants in TLR4 KO mice achieved osteointegration after being placed for 1 week. Less gingival swelling was observed in the ligation group of TLR4 KO mice compared with those in WT mice during the implant healing period (within 14 days) (Fig. 1). The implant appeared completely covered with soft tissue by 42 days. This was not seen in the TLR4 KO mice. Significantly lower bleeding on probing rate was found in the ligation group of TLR4 KO mice compared with those in WT mice ($P < 0.01$, see Supplementary Table 1 in online *Journal of Periodontology*).

### 3.3 | The level of peri-implant bone resorption was reduced in TLR4 KO mice compared with WT mice after *P. gingivalis* infection plus ligation

TLR4 KO mice showed significantly lower bone resorption after ligation compared with those in WT mice detected by both 2D imaging analysis ($P = 0.028$, Figs. 2C and 2E) and μCT analysis ($P = 0.044$, Figs. 2D and 2F) at 14 days post ligation. TRAP staining results showed that significantly higher number of osteoclasts were observed in ligation group versus non-ligation control group in WT and TLR4 KO mice (Figs. 3A and 3B). However, the number of osteoclasts was relatively lower in ligation group in TLR4 KO mice compared with those in WT mice (Fig. 3B). While ligation group showed significantly higher RANKL positive cells percentage and quantities compared with non-ligation group in both WT mice and TLR4 KO mice, there were no significant differences between ligation groups in WT mice versus TLR4 KO mice (Figs. 3C, 3D, and 3E). Moreover, the gingival receptor activator of nuclear factor-kappa B ligand/OPG mRNA ratio (a reflection of the level of osteoclastogenesis) in ligation group was significantly increased compared with non-ligation group in WT mice but not in TLR4 KO mice. There was no significant difference of RANKL/OPG ratio between ligation groups in WT mice versus TLR4 KO mice (Fig. 3F).

### 3.4 | TLR4 KO mice demonstrated reduced inflammatory CD45+ and CD3+ cell infiltration in *P. gingivalis*-associated ligature-induced peri-implantitis

In both WT mice and TLR4 KO mice, significantly higher number of inflammatory cells were found infiltrating around the peri-implant tissues in ligation group compared with the non-ligation group (Figs. 4A and 4B). However, the number of inflammatory cells in tissues of ligation group was significantly lower in TLR4 KO mice compared with those WT mice (Figs. 4A and 4B). Among the inflammatory cells, the lymphocytes were the predominant type of inflammatory cells. Significantly higher number of CD45+ cells (Figs. 4C and 4D) and CD3+ cells (Figs. 4E and 4F) were found in the ligation group when compared with non-ligation group in both WT mice and TLR4 KO mice by immunohistochemistry. Consistently, significantly less CD45+ and CD3+ cells were found in the ligation group of TLR4 KO mice compared with those of the WT mice. However, the increased CD45+ cell infiltration was drastically reduced in TLR4 KO mice (8-fold increase compared with control) compared to those in WT mice (38-fold increase compared with control) (Fig. 4D),

whereas the fold increase of CD3+ cell infiltration in TLR4 KO mice versus WT mice was comparable (8.7-fold versus 8-fold) (Fig. 4F),

### 3.5 | Proinflammatory and anti-inflammatory cytokine expression profile were changed in TLR4 KO mice compared with those in WT mice in *P. gingivalis*-associated ligature-induced peri-implantitis

For IL-1$\beta$, there was no significant difference between ligation group and non-ligation group in WT mice, but significantly higher level of expression in ligation group than in non-ligation group in TLR4 KO mice (Fig. 5A). TNF-$\alpha$ mRNA showed a significant up-regulation in ligation group compared with non-ligation group in WT mice but not in TLR4 KO mice (Fig. 5B). Moreover, TNF-$\alpha$ expression showed significant decrease in TLR4 KO mice compared with those in WT mice after ligation (Fig. 5B). Both IFN-$\gamma$ and IL-17 mRNA showed significant increase in ligation group compared with non-ligation group in TLR4 KO mice but not in WT mice, and significantly higher expression in TLR4 KO mice than WT mice after ligation (Fig. 5C and 5D). For anti-inflammatory factors, IL-10 showed a significant increase in ligation group compared with non-ligation group in WT mice but not in TLR4 KO mice (Fig. 5E). Taken together, TLR4 signaling showed differential regulation on gingival mRNA expression of proinflammatory and anti-inflammatory cytokines in peri-implantitis.

## 4 | DISCUSSION

Multiple animal models have been explored and used in the mechanistic studies of peri-implantitis. Mouse model can be a perfect choice to explore the function of specific pathways in a disease due to the wide availability of transgenic mice. However, the limited size of mouse teeth and alveolar bone can be an obstacle for the use of this animal model. We have recently established a mouse ligation model to study inflammation and alveolar bone loss in experimental peri-implantitis versus periodontitis.[9] The current mouse model used in this study added live *P. gingivalis* infection to establish relevance to human disease and to provide reliable and predictable peri-implantitis parameters including gingival inflammation and bone resorption. Apparent inflammatory responses could be observed after the *P. gingivalis*-soaked ligature was applied around the implants. Similar methods and results are reported by Pirih et al.[22] Two-dimensional imaging analysis, μCT analysis, TRAP staining results together with the RANKL/OPG mRNA ratio results are consistent with each other to indicate cellular and molecular changes leading to the bone resorption. In our experimental peri-implantitis animal model, the bone loss was accessed until 14 days after ligation, indicating later events causing the induction of bone resorption. It would be also helpful to investigate at earlier time points to study early events related to bone loss in the future work. Interestingly, our supplemental data (see Figure S1 in online *Journal of Periodontology*) showed that there was no significant difference in the level of peri-implant bone loss between WT and TLR4 KO mice when comparing respective ligation group versus non-ligation control group at day 7 post ligation. This may indicate that TLR4 signaling is mainly involved at a later stage of peri-implant bone loss.

Our present data showed that significantly greater inflammation of the peri-implant soft tissues was observed in the ligation group of WT mice compared with those in TLR4 KO mice within 14 days (Fig. 1), suggesting that TLR4 may play an essential role for gingival inflammation of peri-implantitis at early stages. Therefore, it is expected that TLR4 signaling also contributes to the early stage bone loss in peri-implantitis. In addition, the implant appeared completely covered with soft tissue by 42 days in WT mice but this was not seen in the TLR4 KO mice (Fig. 1). This may suggest a role of TLR4 in gingival overgrowth during wound healing.

The histologic data demonstrated that infiltrated cells observed were predominantly macrophages, monocular and lymphocytes, which were consistent with Nguyen's results.[23] Previous report indicated that an increased T and B cell local infiltration were found in peri-implantitis soft tissues.[24] Our immunofluorescence staining result demonstrated $CD45^+$ and $CD3^+$ cell infiltration around implant after ligation (Figs. 4C and 4E), which further depicted the subsets of immune T and B cells that are involved in the peri-implantitis inflammatory responses. In particular, the increased infiltration (measured by fold change) of $CD45^+$ cells, but not $CD3^+$ cells, was greatly dampened in TLR4 KO mice compared with WT mice (8-fold versus 38-fold), indicating a TLR4-mediated B cell infiltration in peri-implantitis inflammation and bone loss. B cells are reported to be a well characterized cells for balancing RANKL and OPG ratio by regulating the cytokine productions (such as TNF-$\alpha$) in periodontitis.[25–27] Choi et al. report that B cells can promote or attenuate bone resorption under different background conditions.[28] The TLR4-mediated B cell infiltration observed in this study is likely to shift the balance of RANKL/OPG ratio and TNF-$\alpha$ production and act as a promoter for bone resorption of *P. gingivalis* associated ligature-induced peri-implantitis. Indeed, upregulation of RANKL/OPG ratio (Fig. 3E) and TNF-$\alpha$ (Fig. 5B) observed in WT mice were diminished in TLR4 KO mice. The differences in pathogenesis and disease progression between peri-implantitis and periodontitis may be a reason why the RANKL/OPG ratio was significantly changed between the control group and the *P. gingivalis*-Lig group in the TLR4 KO mice in experimental periodontitis[19] but not in experimental peri-implantitis (Fig. 3E). Additionally, we cannot rule out the possibility that since the variation of RANKL/OPG ratio for the unligated KO mice is high relative to WT controls, inclusion of additional animals could reduce the SEM such that the ratio could increase following ligation. Moreover, it is interesting to observe a relatively high level of RANKL/OPG ratio in unligated KO control compared with WT control (Fig. 3E), of which the underlying biology still need to be determined. Nonetheless, further investigations are needed to understand the detailed characterization of B cells and RANKL/OPG ratio change in TLR4-mediated peri-implantitis.

Gingival TNF-$\alpha$ and IL-10 mRNA was significantly upregulated in *P. gingivalis* associated ligature group when compared with non-ligation control group in WT mice (Figs. 5B and 5F). Recent literature also reports that TNF- $\alpha$ showed up-regulation in *P. gingivalis* infected implants when compared with uninfected implants.[17] TNF-$\alpha$ was reported to play a key role in the LPS induced bone resorption process.[29] Kumar et al. report that significantly up-regulation of TNF-$\alpha$ expression can be observed in CD45 positive lung cells when compared with CD45 negative lung cells when exposed to diesel exhaust particle-induced pulmonary inflammation.[30] Combined with our result, it is reasonable to suggest that TLR4

exacerbates *P. gingivalis* associated ligature induced peri-implantitis bone resorption by up-regulation the TNF-$\alpha$ expression. IL-10, an anti-inflammatory cytokines is reported to delineate up-regulation in periodontitis patients[31] and peri-implantitis murine model.[9] Scholars report that IL-10 is involved in the downregulation of TNF-$\alpha$ expression, and TLR4 can promotes the expression of TNF-$\alpha$ and IL-10 keeping the balance between TNF-$\alpha$ and IL-10.[32] These results are consistent with our TNF-$\alpha$ and IL-10 mRNA results between the WT and TLR4 KO mice. However, we also found upregulated proinflammatory cytokines including IL-1$\beta$, IL-17, and IFN-$\gamma$. IFN-$\gamma$ is reported to suppress the osteoclasts' function,[33] so the upregulation of IFN- $\gamma$ (Fig. 5C) is consistent with our bone resorption result (Fig. 3B) in TLR4 KO mice. Unexpectedly, our data showed that IL-17 mRNA expression was significantly increased in TLR4 KO mice in ligation groups compared with both WT ligation group and KO control group (Fig. 5D). IL-17 was found to be elevated in periodontitis than in gingivitis human samples[34] and stimulated progression of gingivitis to periodontitis in animal models[35] This suggests that although TLR4 deficiency reduce overall inflammation and bone loss in peri-implantitis, such deficiency may also promote certain proinflammatory cytokine productions under pathogenic condition. It is yet to be determined whether IL-17 expression is differentially regulated by TLR4 signaling in periodontitis versus peri-implantitis. Nonetheless, the overall effect of TLR4 pathway regulation on cytokine responses in peri-implantitis and subsequent protective versus pathogenic signal in this process need further investigations. Such information is valuable to design targeted strategies to enhance benefits and alleviate side effects.

## 5 | CONCLUSIONS

In summary, this study suggested that TLR4 signaling mediates inflammation and bone resorption in *P. gingivalis* associated ligature-induced peri-implantitis through regulation of immune B cell infiltration, RANKL/OPG expression ratio, and differential inflammatory cytokine production. Future studies involving in vivo as well as in vitro controlled systems are warranted to delineate potential mechanism of TLR-mediated peri-implantitis pathogenesis.

## Supplementary Material

Refer to Web version on PubMed Central for supplementary material.

## ACKNOWLEDGMENTS

This study was supported by NIH NIDCR grant R01DE023838 to Q Yu and R01DE025255 to X Han.
All affiliations, corporate or institutional, and all sources of financial support to this research are properly acknowledged.

## REFERENCES

1. Brignardello-Petersen R Tooth loss, periodontal disease, and dental caries may be associated with decreased oral health-related quality of life, but there is no evidence about the magnitude of this association. J Am Dent Assoc. 2017;148:e150. [PubMed: 28821339]
2. Bertin TJC, Thivichon-Prince B, LeBlanc ARH, Caldwell MW, Viriot L. Current perspectives on tooth implantation, attachment, and replacement in amniota. Front physiol. 2018;9:1630. [PubMed: 30519190]

3. Mombelli A, Muller N, Cionca N. The epidemiology of peri-implantitis. Clin Oral Implants Res. 2012;23(Suppl 6): 67–76.
4. Khoshkam V, Chan HL, Lin GH, et al. Reconstructive procedures for treating peri-implantitis: a systematic review. J Dent Res. 2013;92:131S–138S. [PubMed: 24158331]
5. Colombo APV, Tanner ACR. The role of bacterial biofilms in dental caries and periodontal and peri-implant diseases: a historical perspective. J Dent Res. 2019;98:373–385. [PubMed: 30890060]
6. Berglundh T, Zitzmann NU, Donati M. Are peri-implantitis lesions different from periodontitis lesions. J Clin Periodontol. 2011;38(Suppl 11):188–202. [PubMed: 21323715]
7. Carcuac O, Abrahamsson I, Albouy JP, Linder E, Larsson L, Berglundh T. Experimental periodontitis and peri-implantitis in dogs. Clin Oral Implants Res. 2013;24:363–371. [PubMed: 23176551]
8. Carcuac O, Berglundh T. Composition of human peri-implantitis and periodontitis lesions. J Dent Res. 2014;93:1083–1088. [PubMed: 25261052]
9. Yu X, Hu Y, Freire M, Yu P, Kawai T, Han X. Role of toll-like receptor 2 in inflammation and alveolar bone loss in experimental peri-implantitis versus periodontitis. J Periodontal Res. 2017.
10. Dabdoub SM, Tsigarida AA, Kumar PS. Patient-specific analysis of periodontal and peri-implant microbiomes. J Dent Res. 2013;92:168S–175S. [PubMed: 24158341]
11. Schminke B, Vom Orde F, Gruber R, Schliephake H, Burgers R, Miosge N. The pathology of bone tissue during peri-implantitis. J Dent Res. 2015;94:354–361. [PubMed: 25406169]
12. Beutler BA. TLRs and innate immunity. Blood. 2009;113:1399–1407. [PubMed: 18757776]
13. Kawai T, Akira S. Toll-like receptors and their crosstalk with other innate receptors in infection and immunity. Immunity. 2011;34:637–650. [PubMed: 21616434]
14. Gursoy UK, He Q, Pussinen P, Huumonen S, Kononen E. Alveolar bone loss in relation to toll-like receptor 4 and 9 genotypes and *Porphyromonas gingivalis* carriage. Eur J Clin Microbiol Infect Dis. Microb. 2016;35:1871–1876.
15. Waller T, Kesper L, Hirschfeld J, et al. *Porphyromonas gingivalis* outer membrane vesicles induce selective tumor necrosis factor tolerance in a toll-like receptor 4- and mTOR-Dependent manner. Infect Immun. 2016;84:1194–1204. [PubMed: 26857578]
16. Oliveira RR, Fermiano D, Feres M, et al. Levels of candidate periodontal pathogens in subgingival biofilm. J Dent Res. 2016;95:711–718. [PubMed: 26936213]
17. Tzach-Nahman R, Mizraji G, Shapira L, Nussbaum G, Wilensky A. Oral infection with *Porphyromonas gingivalis* induces peri-implantitis in a murine model: evaluation of bone loss and the local inflammatory response. J Clin Periodontol. 2017;44:739–748. [PubMed: 28453225]
18. Lin J, Bi L, Yu X, et al. *Porphyromonas gingivalis* exacerbates ligature-induced, RANKL-dependent alveolar bone resorption via differential regulation of Toll-like receptor 2 (TLR2) and TLR4. Infect Immun. 2014;82:4127–4134. [PubMed: 25047844]
19. Lin M, Hu Y, Wang Y, Kawai T, Wang Z, Han X. Different engagement of TLR2 and TLR4 in *Porphyromonas gingivalis* vs. ligature-induced periodontal bone loss. Braz Oral Res. 2017;31:e63. [PubMed: 28832712]
20. Hu Y, Yu P, Yu X, Hu X, Kawai T, Han X. IL-21/anti-Tim1/CD40 ligand promotes B10 activity in vitro and alleviates bone loss in experimental periodontitis in vivo. Biochim Biophys Acta. 2017;1863(9):2149–2157.
21. Yu P, Hu Y, Liu Z, et al. Local induction of B cell interleukin-10 competency alleviates inflammation and bone loss in ligature-Induced experimental periodontitis in mice. Infect Immun. 2017;85(1).
22. Pirih FQ, Hiyari S, Leung HY, et al. A murine model of lipopolysaccharide-induced peri-Implant mucositis and peri-Implantitis. J Oral Implantol. 2015;41:e158–e164. [PubMed: 24967609]
23. Nguyen Vo TN, Hao J, Chou J, et al. Ligature induced peri-implantitis: tissue destruction and inflammatory progression in a murine model. Clin Oral Implants Res. 2017;28:129–136. [PubMed: 26799246]
24. Degidi M, Artese L, Piattelli A, et al. Histological and immunohistochemical evaluation of the peri-implant soft tissues around machined and acid-etched titanium healing abutments: a prospective randomised study. Clin Oral Investig. 2012;16:857–866.

25. Klausen B, Hougen HP, Fiehn NE. Increased periodontal bone loss in temporarily B lymphocyte-deficient rats. J Periodontal Res. 1989;24:384–390. [PubMed: 2531793]
26. Weitzmann MN. The role of inflammatory cytokines, the RANKL/OPG Axis, and the immunoskeletal interface in physiological bone turnover and osteoporosis. Scientifica. 2013;2013: 125705. [PubMed: 24278766]
27. Yun TJ, Chaudhary PM, Shu GL, et al. OPG/FDCR-1, a TNF receptor family member, is expressed in lymphoid cells and is upregulated by ligating CD40. J Immunol. 1998;161:6113–6121. [PubMed: 9834095]
28. Choi Y, Kim JJ. B cells activated in the presence of Th1 cytokines inhibit osteoclastogenesis. Exp Mol Med. 2003;35:385–392. [PubMed: 14646592]
29. Abu-Amer Y, Ross FP, Edwards J, Teitelbaum SL. Lipopolysaccharide-stimulated osteoclastogenesis is mediated by tumor necrosis factor via its P55 receptor. J Clin Invest. 1997;100:1557–1565. [PubMed: 9294124]
30. Kumar S, Joos G, Boon L, Tournoy K, Provoost S, Maes T. Role of tumor necrosis factor-alpha and its receptors in diesel exhaust particle-induced pulmonary inflammation. Sci Rep. 2017;7:11508. [PubMed: 28912506]
31. Escalona LA, Mastromatteo-Alberga P, Correnti M. Cytokine and metalloproteinases in gingival fluid from patients with chronic periodontitis. Invest Clin. 2016;57:131–142. [PubMed: 28429894]
32. Inoue M, Arikawa T, Chen YH, et al. T cells down-regulate macrophage TNF production by IRAK1-mediated IL-10 expression and control innate hyperinflammation. PNAS. 2014;111:5295–5300. [PubMed: 24706909]
33. Nagy E, Lei Y, Martinez-Martinez E, et al. Interferon-gamma released by activated CD8+ T lymphocytes impairs the calcium resorption potential of osteoclasts in calcified human aortic valves. Am J Pathol. 2017;187:1413–1425. [PubMed: 28431214]
34. Thorbert-Mros S, Larsson L, Kalm J, Berglundh T. Interleukin-17 producing T cells and interleukin-17 mRNA expression in periodontitis and longstanding gingivitis lesions. J Periodontol. 2019;90:516–521. [PubMed: 30536765]
35. Sommer MEL, Dalia RA, Nogueira AVB, et al. Immune response mediated by Th1/IL-17/caspase-9 promotes evolution of periodontal disease. Arch Oral Biol. 2019;97:77–84. [PubMed: 30366216]

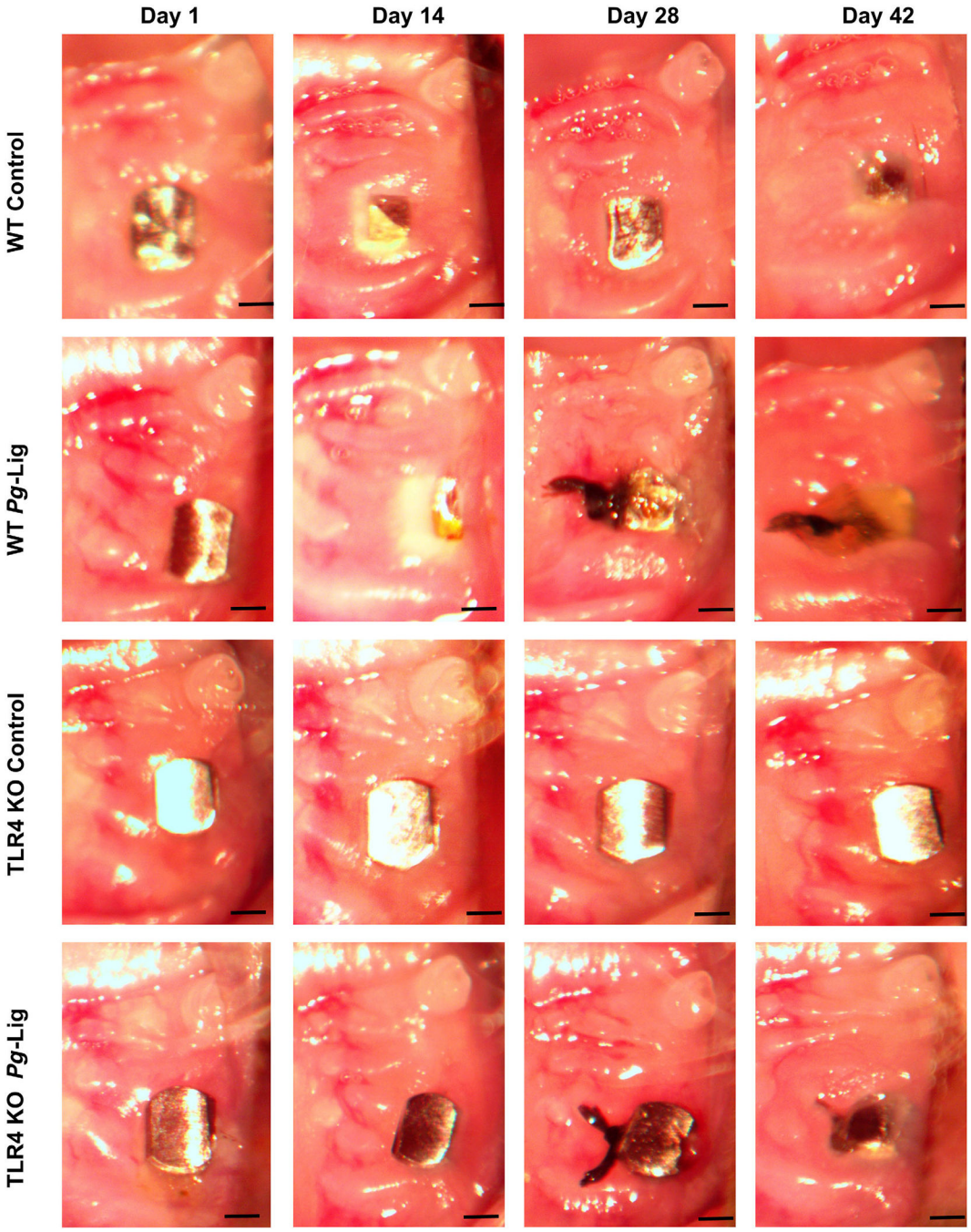


**FIGURE 1.**

Clinical observation and evaluation of implants at different time points (day 1, 14, 28, and 42 after implants placement). The placed implants achieved integrity 28 days after being placed in WT mice. Gingival tissue around the implants showed pink in color, no obviously red gingiva swelling and bleeding on probing observed on day 28. The *P. gingivalis* associated ligature induced severe gingiva swelling compared with control after being applied for 14 days at day 42. Implants in TLR4 KO group also displayed integrity on day 28. The gingival swelling and bleeding on probing induced by *P. gingivalis* associated

ligature showed less in TLR4 KO mice compared with those in WT mice by observations (scale bar, 500 μm)

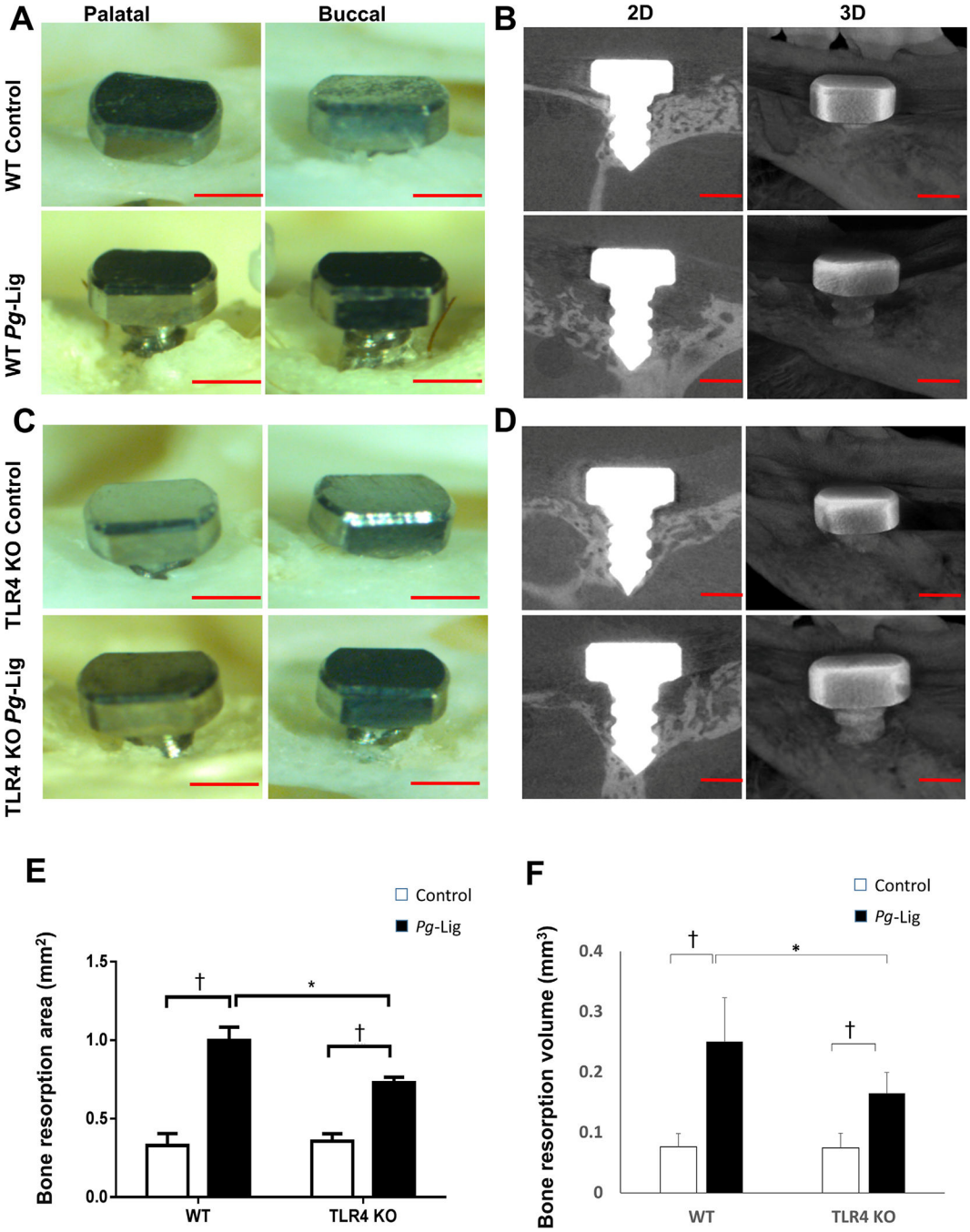


**FIGURE 2.**

*P. gingivalis* associated ligature-induced bone resorption was measured in WT and TLR4 KO mice. Palatal and buccal side images of the defleshed skulls were taken of *P. gingivalis* associated ligature (*Pg*-Lig) group and non-ligation (control) group in WT mice (**A**) and TLR4 KO mice (**C**) (scale bar, 500 μm). The bone resorption area based on these images were measured and analyzed (**E**) (mean ± SEM, n = 6, $^{*}P < 0.05$, $^{\dagger}P < 0.01$, SEM, standard error of difference between two means). Three-dimensional (3D) images from μCT were

collected for WT mice (**B**) and TLR4 KO mice (**D**) (scale bar, 500 μm) and analyzed (**F**) (mean ± SEM, n = 6, *$P < 0.05$, †$P < 0.01$)

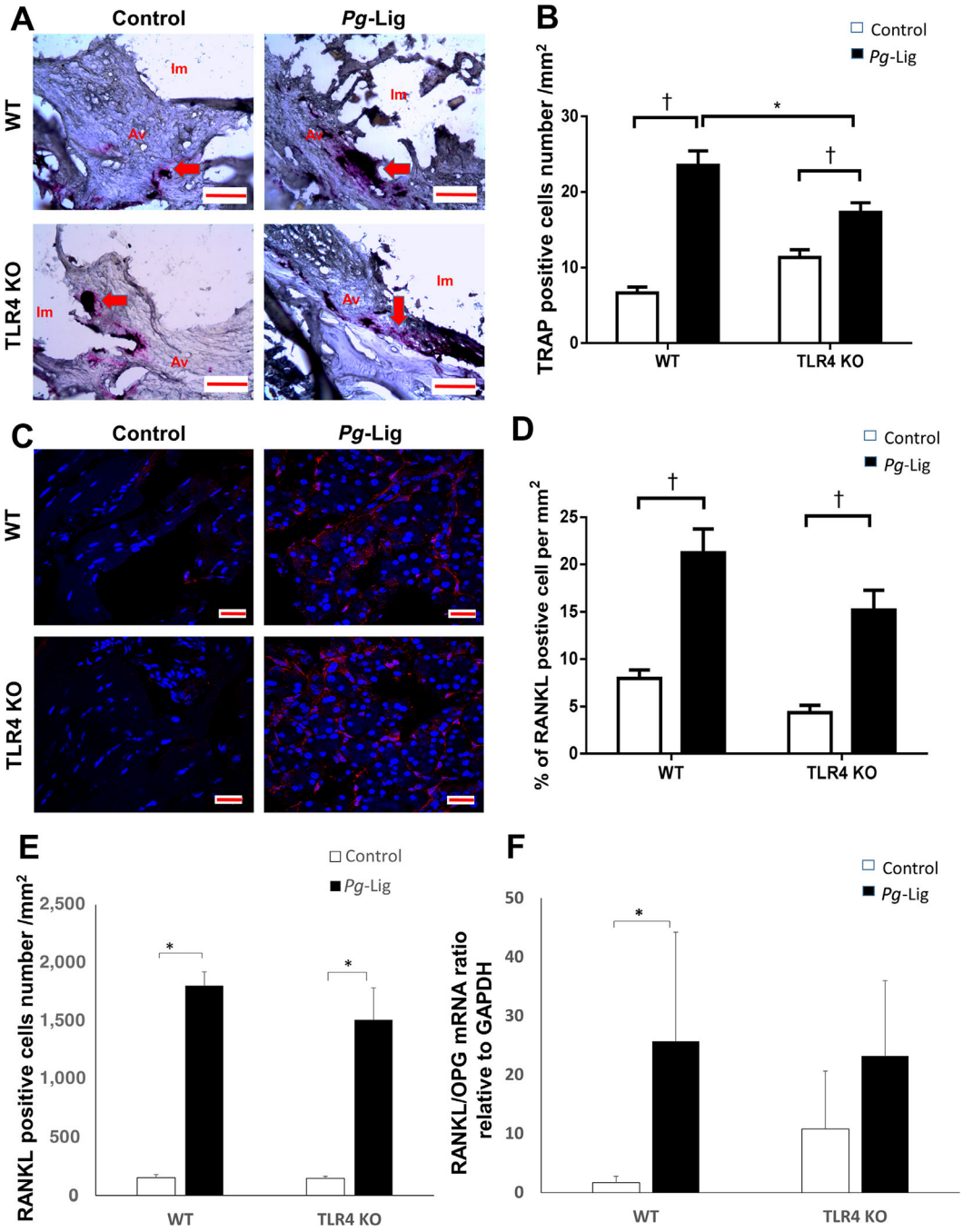


**FIGURE 3.**

TRAP positive, RANKL positive cells and gingival RANKL/OPG mRNA ratio were increased in the *P. gingivalis* associated ligature-induced peri-implantitis in WT mice. TRAP positive cells (red color) with ≥3 nuclei were considered osteoclasts and were shown in control group and *P. gingivalis* (*Pg*)-Lig group of both WT mice and TLR4 KO mice (**A**, red arrows) (i.m., implant space; a.v., alveolar bone; scale bar, 100 μm) and analyzed (**B**) (mean ± SEM, n = 5, $^{*}P < 0.05$, $^{\dagger}P < 0.01$). The RANKL immunofluorescence staining positive cells were shown in control and *Pg*-Lig group of both WT mice and TLR4 KO mice (**C)**

(Scale bar, 20 μm) and analyzed by percentages of the positive staining cell per $mm^2$ (**D**) or positive cells numbers per $mm^2$ (**E**) (mean ± SEM, n = 5, $^{*}P < 0.05$, $^{\dagger}P < 0.01$). Gingiva mRNA RANKL/OPG ratio was measured and analyzed in control group and *Pg*-Lig group of both WT mice and TLR4 KO mice (**F**) (mean ± SEM, n = 6, $^{*}P < 0.05$)

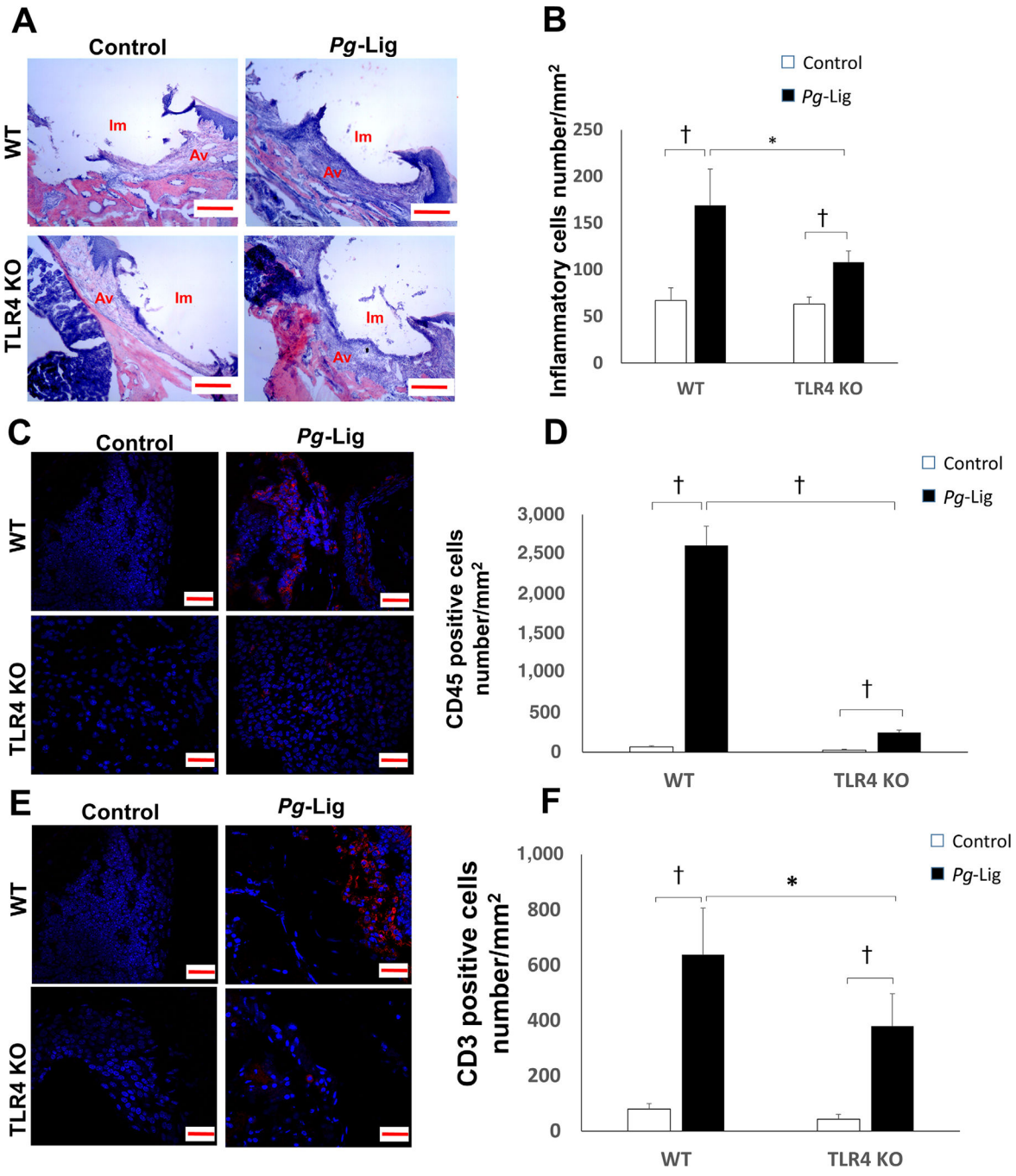


**FIGURE 4.**

The inflammatory cell infiltration of the implants gingival tissues was increased in the *P. gingivalis* associated ligature-induced peri-implantitis in WT and TLR4 KO mice. H&E staining of the gingival tissue around implants was performed in control group and *P. gingivalis* (*Pg*)-Lig group of both WT mice and TLR4 KO mice (**A**) (i.m., implant space; a.v., alveolar bone; scale bar, 200 μm). Inflammatory cells number were measured and analyzed in each group (**B**) (mean ± SEM, n = 5, $^{*}P < 0.05$, $^{\dagger}P < 0.01$). CD45 immunofluorescence staining positive cells (red color) were shown in control and *Pg*-Lig

group of both WT mice and TLR4 KO mice (**C**) (Scale bar, 20 μm) and analyzed (**D**) (mean ± SEM, n = 5, $^{\dagger}P < 0.01$). CD3 immunofluorescence staining positive cells (red color) were shown in control and *Pg*-Lig group of both WT mice and TLR4 KO mice (**E**) and analyzed (**F**) (mean ± SEM, n = 5, $^{*}P < 0.05$, $^{\dagger}P < 0.01$)

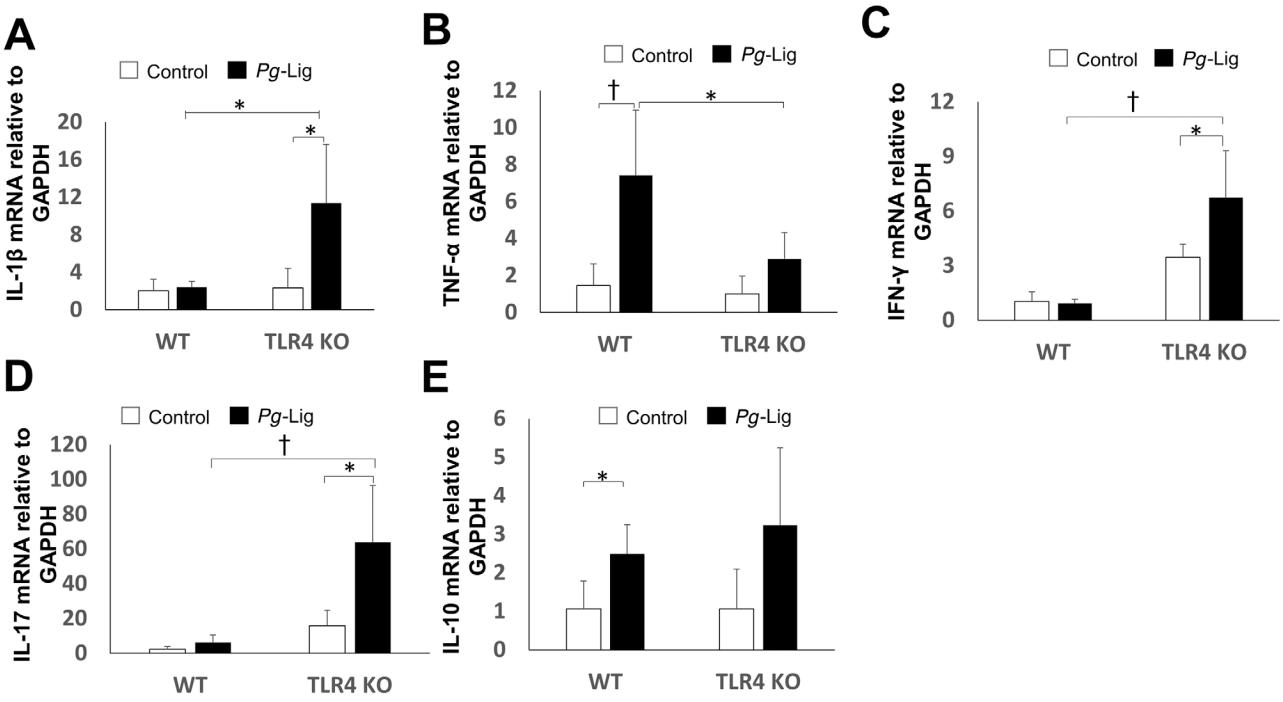


**FIGURE 5.**

Gingival proinflammatory and anti-inflammatory cytokines mRNA expression changes in the *P. gingivalis* associated ligature-induced peri-implantitis in WT and TLR4 KO mice. Gingival tissues around ligatured implants and non-ligation implants were excised and processed for RT-qPCR analyses to determine mRNA level of IL-1$\beta$ (**A**), TNF-$\alpha$ (**B**), IFN-$\gamma$ (**C**), IL-17(**D**), and IL-10 (**E**) (mean ± SEM, n = 6, *$P < 0.05$, $^{\dagger}P < 0.01$)

**TABLE 1**

The sequences of primers used in RT-qPCR

| Gene | Orientation | Sequence |
|---|---|---|
| GAPDH | Forward | 5′-CCCCAGCAAGGACACTGAGCAA-3′ |
| | Reverse | 5′-GTGGGTGCAGCGAACTTTATTGATG-3′ |
| IL-1$\beta$ | Forward | 5′-CCAGCTTCAAATCTCACAGCAG-3′ |
| | Reverse | 5′-CTTCTTTGGGTATTGCTTGGGATC-3′ |
| IL-10 | Forward | 5′-TGGCCCAGAAATCAAGGAGC-3′ |
| | Reverse | 5′-CAGCAGACTCAATACACACT-3′ |
| IL-17 | Forward | 5′-AACACTGAGGCCAAGGACTT-3′ |
| | Reverse | 5′-ACCCACCAGCATCTTCTCG-3′ |
| TNF-$\alpha$ | Forward | 5′-CACAGAAAGCATGATCCGCGACGT-3′ |
| | Reverse | 5′-CGGCAGAGAGGAGGTTGACTTTCT-3′ |
| IFN-$\gamma$ | Forward | 5′-GGCCATCAGCAACAACATAAGCGT-3′ |
| | Reverse | 5′-TGGGTTGTTGACCTCAAACTTGGC-3′ |
| RANKL | Forward | 5′-GGGTGTGTACAAGACCC-3′ |
| | Reverse | 5′-CATGTGCCACTGAGAACCTTGAA-3′ |
| OPG | Forward | 5′-AGCAGGAGTGCAACCGCACC-3′ |
| | Reverse | 5′-TTCCAGCTTGCACCACGCCG-3′ |